ENVIRONMENTAL RESEARCH
LETTERS

LETTER • OPEN ACCESS

Unprecedented drought in South India and recent water scarcity

IOP Publishing Environ. Res. Lett. 16 (2021) 054007 https://doi.org/10.1088/1748-9326/abf289

ENVIRONMENTAL RESEARCH
LETTERS

LETTER

Unprecedented drought in South India and recent water scarcity

Vimal Mishra[1,2,*], **Kaustubh Thirumalai**[3], **Sahil Jain**[1] and **Saran Aadhar**[1]

[1] Civil Engineering, Indian Institute of Technology (IIT) Gandhinagar, Gandhinagar, Gujarat 382355, India
[2] Earth Sciences, Indian Institute of Technology (IIT) Gandhinagar, Gandhinagar, Gujarat 382355, India
[3] Department of Geosciences, University of Arizona, 1040 E. 4th Street, Tucson, AZ 85721, United States of America
[*] Author to whom any correspondence should be addressed.

E-mail: vmishra@iitgn.ac.in

Keywords: drought, GRACE, climate variability, water scarcity

Supplementary material for this article is available online

OPEN ACCESS

RECEIVED
25 November 2020

REVISED
11 March 2021

ACCEPTED FOR PUBLICATION
26 March 2021

PUBLISHED
16 April 2021

Abstract

Peninsular Indian agriculture and drinking water availability are critically reliant on seasonal winter rainfall occurring from October to December, associated with the northeastern monsoon (NEM). Over 2016–2018, moderate-to-exceptionally low NEM rainfall gave rise to severe drought conditions over much of southern India and exacerbated water scarcity. The magnitude and dynamics of this drought remain unexplored. Here, we quantify the severity of this event and explore causal mechanisms of drought conditions over South India. Our findings indicate that the 3-year cumulative rainfall totals of NEM rainfall during this event faced a deficit of more than 40%—the driest 3-year period in ∼150 years according to the observational record. We demonstrate that drought conditions linked to the NEM across South India are associated with cool phases in the equatorial Indian and Pacific Oceans. Future changes in these teleconnections will add to the challenges of drought prediction.

1. Introduction

Deficiency of the summer monsoonal precipitation is one of the main drivers of meteorological drought in India, which if prolonged, can transform into more impactful agricultural and hydrological droughts (Mishra and Singh 2010, Mishra *et al* 2010, Mo 2011). Agricultural and hydrological droughts can pose lasting impacts on food production and water availability, respectively (Van Loon 2015, Samaniego *et al* 2018, Mishra 2020). India experiences two major monsoon seasons—the Indian summer monsoon (ISM), also known as the southwestern monsoon and the lesser-studied northeastern monsoon (NEM) or the winter monsoon (Gadgil and Gadgil 2006, Rajeevan *et al* 2012). The ISM is the major source of precipitation for much of India over the period of June to September (hereafter JJAS) and has been the focus of extensive study (Gadgil and Gadgil 2006, Singh *et al* 2019). On the other hand, the NEM is more important in selected parts of India and is associated with rainfall during the period between October and December (hereafter OND) (Kripalani and Kumar 2004, Zubair and Ropelewski 2006, Yadav 2012). In particular, the NEM significantly impacts peninsular India, where certain parts of South India receive a majority of their annual rainfall totals during the OND season (Rajeevan *et al* 2012). Despite lesser precipitation totals compared to the ISM, the NEM is critically important for water availability, agriculture, and the livelihood of millions of people residing in peninsular India.

Previously, studies have indicated that both monsoon seasons have experienced profound changes over the past few decades (Mishra *et al* 2012, Rajeevan *et al* 2012, Roxy *et al* 2015, Singh *et al* 2019). For instance, seasonal mean precipitation associated with the ISM has shown a declining trend leading to more frequent monsoon-season deficits (Mishra *et al* 2012, Christensen *et al* 2013, Roxy *et al* 2015). Similarly, the increase in precipitation associated with the NEM over the last few decades has been attributed to the warming of the Indian Ocean (Mishra *et al* 2012, Roxy *et al* 2015). Furthermore, the El Niño Southern Oscillation (ENSO) and Indian Ocean Dipole (IOD) phenomena are well-known drivers of deficits in monsoon rainfall (Ashok *et al* 2001, Kumar *et al* 2007) and are also expected to undergo changes with ongoing increases in greenhouse gases (Cai *et al* 2018, Timmermann *et al* 2018). Addressing

the mechanisms of why and how these monsoon seasons are shifting under a warming world is critical for improving predictions of drought conditions in India.

Whereas previous studies have shown strong linkages between summer monsoon droughts in India and sea surface temperature (SST) variability in the equatorial Indian and Pacific Oceans (Kripalani and Kulkarni 1997, Barlow *et al* 2002, Niranjan Kumar *et al* 2013, Roxy *et al* 2015), few studies have focused on the causes of rainfall deficits associated with the NEM (Dimri *et al* 2016). From 2016 to 2018, South India witnessed severe drought conditions, which significantly impacted agriculture and water availability in the region ('Chennai water crisis: City's reservoirs run dry,' BBC 2019). The densely populated states of Andhra Pradesh, Karnataka, and Tamil Nadu continuously declared drought in 2016, 2017, and 2018 related to the deficits in NEM precipitation. The drought caused water crises in both urban and rural areas (Aguilera 2019). Despite the profound impacts of the 2016–18 drought in South India, its magnitude, drivers, and mechanisms remain unexplored. In this study, we focus on the 2016–2018 drought, quantify its severity, and investigate its causes and relationships with regional and global ocean–atmosphere variability. We place this extreme event in the context of the previous droughts and conclude that its severity was unprecedented over the observational record.

2. Data and methods

The NEM (October–December) is a dominant source of rainfall in South India (Rajeevan *et al* 2012). South India (Latitude: 8°N–15°N; Longitude: 74°E–81°E)) comprises of five Indian states and three union territories. The region encompasses nearly 19% of India's area and harbors around 250 million people, which is one-fifth of the total population of India (Census of India 2011). South India is an agriculturally rich part of the country, with over 60% of its rural population engaged in agriculture (Aulong *et al* 2012). The population depends largely on the NEM for agricultural production. We used gridded daily precipitation data available at 0.5° spatial resolution for the period of 1870–2018 (Mishra *et al* 2019). Mishra *et al* (2019) used station observations from India Meteorology Department (IMD) to develop the gridded precipitation for the pre-1900 (1870–1900) period, which was merged with the gridded data available for the post-1900 period (1901–2018; (Pai *et al* 2014)) from IMD. More details on the gridded precipitation data and evaluation of its quality can be obtained from Mishra *et al* (2019). The gridded data capture orographic precipitation along the Western Ghats, Northeast, and the foothills of Himalaya (Pai *et al* 2014, Mishra *et al* 2019).

Total water storage (TWS) data were obtained from the Gravity Recovery and Climate Experiment (GRACE) and GRACE follow on (GRACE-FO) missions. TWS is available for the period April 2002 to June 2017 from the GRACE satellites. The GRACE-FO mission provides the data from June 2018 to present. Therefore, the TWS data for July 2017 to May 2018 is not available. We obtained TWS from GRACE and GRACE-FO from NASA's Jet Propulsion Lab (JPL: https://podaac.jpl.nasa.gov/dataset/TELLUS_GRAC-GRFO_MASCON_CRI_GRID_RL06_V2) for the 2002–2019 period. The GRACE mascon product (RL06 V2) contains gridded monthly global water storage anomalies relative to mean, which is available at 0.5° spatial resolution (Wiese *et al* 2016). To remove the seasonal cycle from TWS, monthly mean TWS was removed from each month, and scale factors were applied.

To assess the influence of SSTs on the 2016–18 drought, we used monthly data from the HadSST dataset (Hadley Centre) for the period 1870–2018 at 2.0° spatial resolution (Rayner *et al* 2003). We obtained surface air temperatures (SATs) from Berkley Earth (Rohde *et al* 2013) to analyze anomalous temperature conditions during NEM droughts. Since SST data has a strong warming trend, we used Ensemble Empirical Mode Decomposition (EEMD; (Wu and Huang 2009)) to remove the secular trend (Wu *et al* 2011) from SST time series as in Mishra (2020). The EEMD method has an advantage over conventional detrending as it removes both linear and non-linear trends (Mishra 2020). We estimated SST and precipitation anomalies for the NEM (October–December) to diagnose the linkage between precipitation and SST. To examine the coupled variability of precipitation and SST, we use maximum covariance analysis (MCA; (Bretherton *et al* 1992)). In addition, we used empirical orthogonal function (EOF) analysis to obtain the dominant modes of variability in rainfall during the NEM when SST was not used. The MCA, performed on two fields (here precipitation and SST) together, identifies the leading modes of variability in which the variations of the two fields are strongly coupled (Mishra *et al* 2012). Sea level pressure (SLP) and wind fields (horizontal, u and meridional, v) were obtained from the European Centre for Medium-Range Weather Forecasts Reanalysis version 5 (ERA-5; (Hersbach and Dee 2016)) for the period 1979–2018 to understand the mechanism of the northeast monsoon. Further, SLP and wind fields were regridded to 2° to make them consistent with SST.

Towards predictability of NEM rainfall, we employed univariate and multivariate techniques. We use the lagged relationship between SST anomalies and rainfall over South Asia during the NEM as a predictor of OND rainfall. We used SST anomalies from the Nino 3.4 region and over the northern Indian Ocean (NIO; 6°–24°N, 40°–100°E) as a predictor of monthly NEM precipitation using the following three equations:

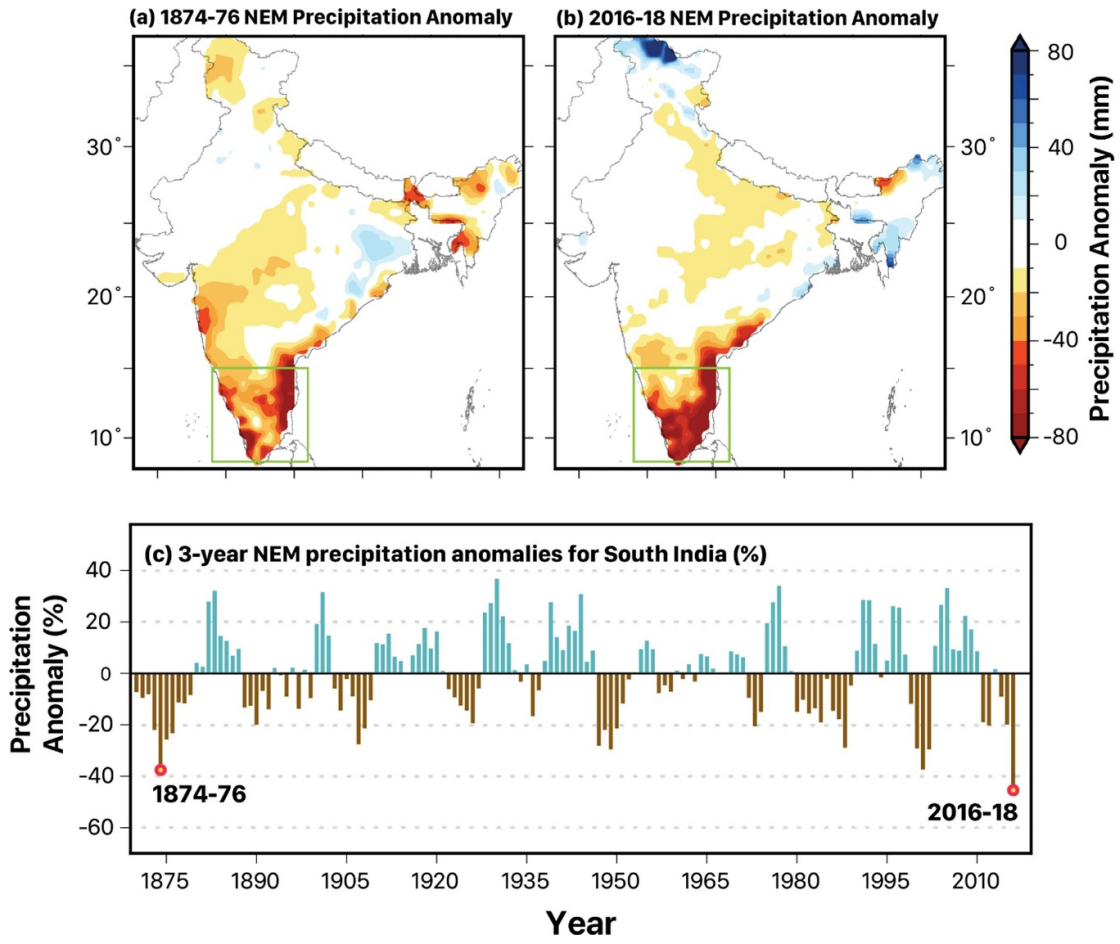

Figure 1. Three-year cumulative precipitation anomalies (mm) during the Northeast monsoon (NEM, October–December). (a), (b) The spatial pattern of 3 year cumulative precipitation anomalies (mm) during 1874–1876 and 2016–2018 periods, respectively, in southern India (denoted by the green box). (c) Area-averaged (over the green box) 3 year moving-mean precipitation anomalies (%) for the period 1870–2016. Red dots in (c) demarcate the two periods of interest, and show that the 2016–18 was the 1st and 1874–76 was the 2nd worst drought in last 150 years. Long-term precipitation data is based on station observations from the Indian Meteorological Department (IMD).

$$R_{\mathrm{OND}} = a^{*}\mathrm{Nino3.4}_{\mathrm{AMJ}} + \varepsilon \quad (1)$$

$$R_{\mathrm{OND}} = a^{*}\mathrm{SST\text{-}NIO}_{\mathrm{OND}} + \varepsilon \quad (2)$$

$$R_{\mathrm{OND}} = a^{*}\mathrm{Nino3.4}_{\mathrm{AMJ}} + \mathrm{SST\text{-}NIO}_{\mathrm{OND}} + \varepsilon. \quad (3)$$

where R_{OND} is rainfall during October-December (OND) over South India, $\mathrm{Nino3.4}_{\mathrm{AMJ}}$ is April-June (AMJ) SST anomalies over the Nino 3.4 region, $\mathrm{SST\text{-}NIO}_{\mathrm{OND}}$ is SST anomalies during OND over the northern Indian Ocean (NIO), a and b are the regression coefficients, and ε is the residual.

3. Results

3.1. Unprecedented recent failure of northeast monsoon rainfall

South India receives more than 40% of its total annual precipitation during the NEM season (figure S1 (available online at stacks.iop.org/ERL/16/054007/mmedia)), and thus deficits in NEM rainfall pose significant water-related challenges in the region. To investigate the long-term observational history of NEM rainfall in the region, we used rainfall observations from the IMD (Pai *et al* 2014), spanning from 1870 to 2018. Domain-averaged precipitation anomalies associated with the NEM indicate that most of South India experienced exceptional (>40%) precipitation deficits during 1874–1876 and 2016–2018 (figure 1). We calculated precipitation anomalies during the NEM for one, two, and three consecutive year durations over the 1870–2018 period to estimate abnormal deficit-years in the long-term record (figures 1, 2 and S4, table 1). There are five pronounced periods of drought (>29% deficits) in the overall record including the recent drought of 2016–2018, the droughts during 2001–03, 1949–1951, 2002–04, and the well-known Great Drought of 1876–78 (Cook *et al* 2010, Singh *et al* 2018), which was associated with the Great Madras Famine (Blanford 1884, Mishra *et al* 2019). Among these events, our analysis indicates that the Great Drought and the recent event of 2016–18 are the most severe (figure 1). During 2016–18, South India experienced the worst NEM drought over the last 150 years with

Table 1. Top five driest years for one, two, and three-year cumulative northeast monsoon (OND).

		2 year cumulative		3 year cumulative	
Drought year	Precipitation anomaly (%)	Drought year	Precipitation anomaly (%)	Drought year	Precipitation anomaly (%)
1876	−68.82	1875–76	−54.37	2016–18	−45.40
2016	−62.84	2016–17	−51.73	1874–76	−37.52
1938	−59.71	1988–89	−41.29	2001–03	−29.56
1988	−53.74	2002–03	−39.50	1949–51	−29.55
1974	−49.31	1908–09	−37.91	2002–04	−29.55

a precipitation deficit of 45%, whereas the 1874–76 drought was the second-worst, with a deficit of 37% (table 1). We note that the 1-year and 2-year duration NEM deficits for 1876 (69%) and 1876–77 (54%) were comparable to the deficits during 2016 (63%) and the 2016–17 (52%) durations (table 1, figures S2–S4). However, the consecutive 3-year NEM deficit for 2016–18 was more significant than the Great Drought. We find that annual rainfall anomalies additionally indicate drought conditions in 2016, 2017, and 2018 (figure S5). Moreover, 2 and 3-year annual rainfall anomalies for 2016–17 and 2016–18 also show a major rainfall deficit in South India (figure S5). Thus, we conclude that the 2016–18 drought caused by the failure of the NEM also contained severe annual rainfall deficits.

Over individual NEM seasons, the two most extreme dry events occurred in 1876 and 2016 with precipitation deficits of 69% and 63%, respectively (table 1). The rainfall deficit in 2016 was more severe in comparison to the lack of precipitation in 2017 and 2018 (figure S2). The failure of the NEM in 2016 as well as relatively low rainfall totals over the consecutive years were the main causes behind the 2016–18 drought in South India (table 1). Overall, the 3-year NEM drought of 2016–2018 was more severe than the Great Drought of 1874–1876. Infamously, the 1876 drought resulted in famine and the deaths of millions of people (Mishra *et al* 2019, Mishra 2020). The more recent 2016–18 NEM drought considerably influenced water availability in the region and caused a water crisis across South India ('Chennai water crisis: City's reservoirs run dry,' BBC 2019).

Furthermore, the 2016–2018 NEM drought in South India was unprecedented in the last 150 years and had severe implications for water availability. TWS from the GRACE and GRACE–FO satellites showed a considerable loss in South India due to the recent (2016–2018) drought (figure 2). Twelve months moving precipitation anomalies pinpoint the onset of drought in South India during October 2016 and show that it continued till October 2018 (figure 2). Although there was a weak recovery from drought conditions for two months in November and December 2018, these rainfall totals were not enough to negate the influence of the overall event (2016–2018), which continued till August 2019 (figure 2), and was only alleviated by stronger NEM rains later that year. We also note that 12-month precipitation anomalies and TWS anomalies are well-correlated ($r = 0.63$), where local observations indicate that rainfall is the major contributor of TWS (Asoka *et al* 2017). Thus, we attribute the loss in regional TWS to the long-term 3-year drought, which was precipitated by the lack of NEM rainfall.

Total water loss in South India estimated from the GRACE satellite was 79 km^3 in December 2016 (figure 2(a)). Similarly, GRACE–FO data reveal that total water loss in June 2017 and 2019 was 46.5 and 41.7 km^3, respectively (figures 2(b) and (c)). Recovery in TWS occurred in late 2019 due to improved NEM rainfall over the region. The 2016–2018 drought caused a significant loss in TWS, which also likely resulted in a significant depletion in groundwater across South India. We caveat that we did not estimate the overall loss in groundwater due to uncertainty in soil moisture (Long *et al* 2013, Castle *et al* 2014)—an estimate outside the scope of this work—however we suspect that the groundwater depletion was driven by the drought in addition to increased groundwater extraction (Thomas *et al* 2017) during the drought (Asoka *et al* 2017). Despite the uncertainty in the estimation of total water loss from GRACE satellites (Long *et al* 2013), the combined influence of depletion in surface-water and groundwater during this event led to unprecedented water scarcity in South India (Aguilera 2019, 'Chennai water crisis: City's reservoirs run dry,' BBC 2019).

3.2. Mechanism of deficit during the Northeast monsoon

We examined circulation patterns to understand mechanisms behind variability in NEM rainfall. To do so, we first examined climatological surface temperatures (SAT and SST), sea-level pressure (SLP), and wind fields at 850 hPa during the OND season (figure 3). SLP and wind fields were taken from the ERA-5 reanalysis dataset (Hersbach and Dee 2016) whereas SSTs and SATs were taken from HadSST (Rayner *et al* 2003) and Berkley Earth (Rohde *et al* 2013), respectively. Climatologically during boreal fall, cooling SATs over the northwestern Pacific and northern latitudes alongside comparatively warmer mean-annual SSTs over the northern Indian Oceans set up easterly wind flow across the Bay of Bengal (figures 3(a) and (b)). In particular, warm SSTs in the

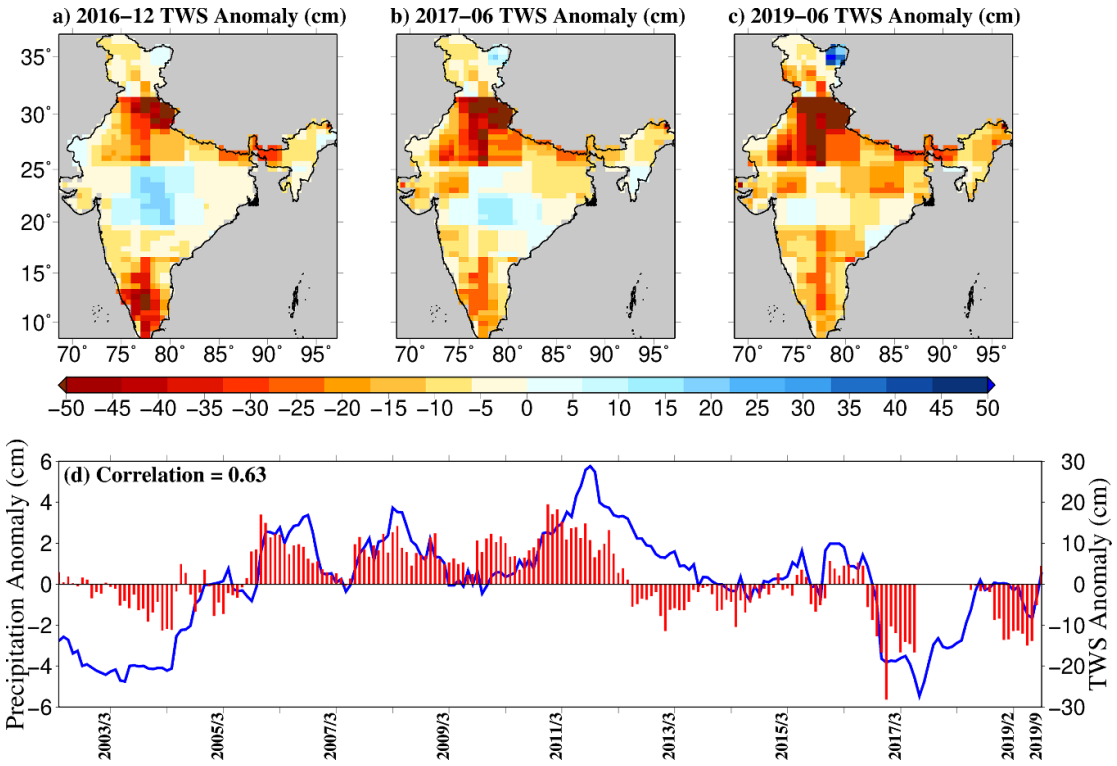

Figure 2. Total water storage (TWS) anomalies from the GRACE and GRACE–FO during 2002–2019. (a)–(c) TWS anomalies (cm) during December 2016, June 2017, and June 2019. (d) 12-month moving-sum precipitation anomalies (cm, in blue) and monthly TWS anomalies (cm, in red) aggregated over South India (south of 15°N). Note that the July 2017 to May 2018 period contains missing data as the GRACE-FO dataset is only available from June 2018 onwards. The Pearson correlation coefficient between TWS anomalies and precipitation anomalies is 0.63.

western Indian Ocean can elicit easterlies across the Indian Ocean and favor moisture transport from the Bay of Bengal into peninsular India. These moisture-bearing winds, which become northeasterly before landfall, bring NEM rainfall to South India (Rajeevan *et al* 2012). Strong winds from across the South China Sea, driven by the underlying SAT and SLP patterns ultimately facilitate NEM rainfall. Thus, El-Niño-like conditions in the Pacific with cooler SSTs in the northern portion of the western tropical Pacific Ocean, juxtaposed with cooler SSTs in the eastern Indian Ocean and warmer SSTs in the west (i.e. resembling positive IOD-like conditions), all serve to enhance NEM rainfall over South India. It is to be expected that circulation patterns which weaken these processes ought to yield diminished NEM rainfall.

To better understand the causes of rainfall deficits, we investigated anomalous patterns during the NEM season for 2016, 2017, and 2018 (figure 3). In 2016 and 2017, as expected, cool SST anomalies prevailed in the tropical Indo-Pacific and were associated with La Niña conditions in the central Pacific along with negative IOD-like conditions in the Indian Ocean (figures 3(c)–(f)). Both years witnessed anomalously cooler SSTs in the eastern tropical Indian Ocean and western tropical Pacific, and warmer SSTs in the western Indian Ocean and central Pacific. These SST patterns, alongside SLP and adjacent continental SAT patterns, gave rise to anomalous westerlies in the equatorial Indian Ocean, which weakened moisture transport from the Bay of Bengal during the NEM season of both events (figures 3(c)–(f)). Moreover, both years were associated with anomalously low SLP and cooler surface temperatures across the Indian subcontinent and Bay of Bengal, sustaining an anomalous anticyclonic pattern which inhibited moisture transport into South India (figures 3(c)–(f)). In 2018, the rainfall deficit conditions were slightly alleviated due to favorable warm conditions in the western tropical Indian Ocean and cooling in the East (development of a positive IOD event) alongside the development of El-Niño-conditions in the Pacific. However, it should be noted that western Indian Ocean warming was not particularly pronounced that year and alongside cooler temperature anomalies in the northern Indian Ocean, resulted in an overall deficit in NEM rainfall that year.

Next, we analyzed surface temperature and precipitation anomalies for the five most severe dry events in South India over the 1870–2018 period during the NEM season (figure 4). The major droughts in South India occurred in 1876, 2016, 1938, 1988, and 1974 (in order of severity). Out of these five droughts, four occurred during La Niña conditions. In contrast, the well-studied drought of 1876 during the NEM was linked with El Niño (figure 4)—a finding reported previously (Cook *et al* 2010, Singh

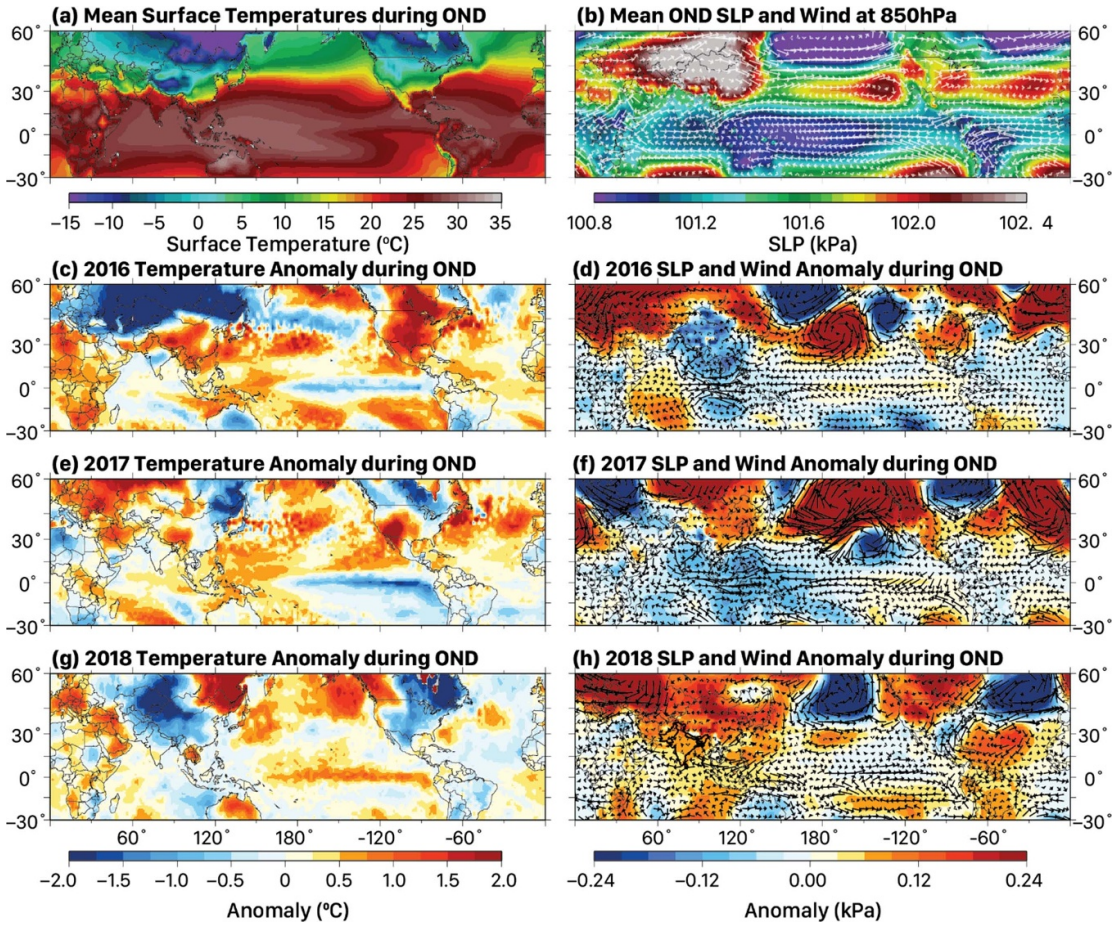

Figure 3. Atmospheric and oceanic patterns during the 2016–18 drought in South India. (a), (b) Climatological mean surface-air temperature (SAT, °C) and sea-surface temperature (SST, °C), mean sea-level pressure (SLP, Pa) and wind at 850 hPa (in (b)) during the October–December (OND) season. (c), (d) SST, SLP, and wind anomalies associated with the NEM during the OND season of 2016, (e), (f) 2017, and (g), (h) 2018. Mean SLP and wind fields were obtained from ERA-5 whereas SST was taken from HadSST and SAT from BEST.

et al 2018, Mishra *et al* 2019). However, it should be noted that cool SST conditions prevailed in the Pacific Ocean over the 1870–1876 period and the transition from the cool to warm phase occurred during the NEM season of 1876 (Singh *et al* 2018). Additionally, the western Indian Ocean was not anomalously warm as it typically is during El Niño years (figure 4(a)). Nevertheless, temperature and SLP anomaly composites for the most severe dry and wet NEM years reveal a general propensity for cooler SSTs in the Indo–Pacific (i.e. La Niña conditions) to be associated with precipitation deficits over South India (figures S6 and S7). On the other hand, warming in the central Pacific and Indian Oceans is associated with a stronger NEM and surplus precipitation (figure S7). Overall, OND cooling in the Indian and central Pacific oceans results in lower SLP and weaker wind fields, which ultimately drive rainfall deficits in South India.

3.3. SST variability during Northeast Monsoon

To clarify the relationship between SST and precipitation anomalies associated with the NEM, we performed MCA, which helps delineate the leading patterns responsible for co-variability between South Indian NEM rainfall and tropical SSTs. The first leading mode exhibits typical ENSO-like patterns of covariance and explains 77.2% of total variance (figure 5(a)). As demonstrated above with patterns of the major droughts (figure 4), MCA also indicates that negative SST anomalies over the central Pacific (i.e. La Niña) and Indian Oceans (negative IOD) result in below normal NEM precipitation over South India (figure 5(b)). The second leading mode of MCA exhibits a relatively weaker relationship between precipitation and SST anomalies during the NEM (figure 5). The second mode fingerprints the role of SST warming in the Indian Ocean as a driver of increased NEM precipitation in South India (Roxy *et al* 2015). We also note that there appears to be a slight dichotomy between northern and southern South India, where NEM precipitation in the latter region is more strongly linked with ENSO (figure 5). On the other hand, precipitation over the northern parts of South India is more strongly associated with the second leading mode (figure 5). This finding might help explain some of the ambiguity surrounding the mechanisms of the impact of the

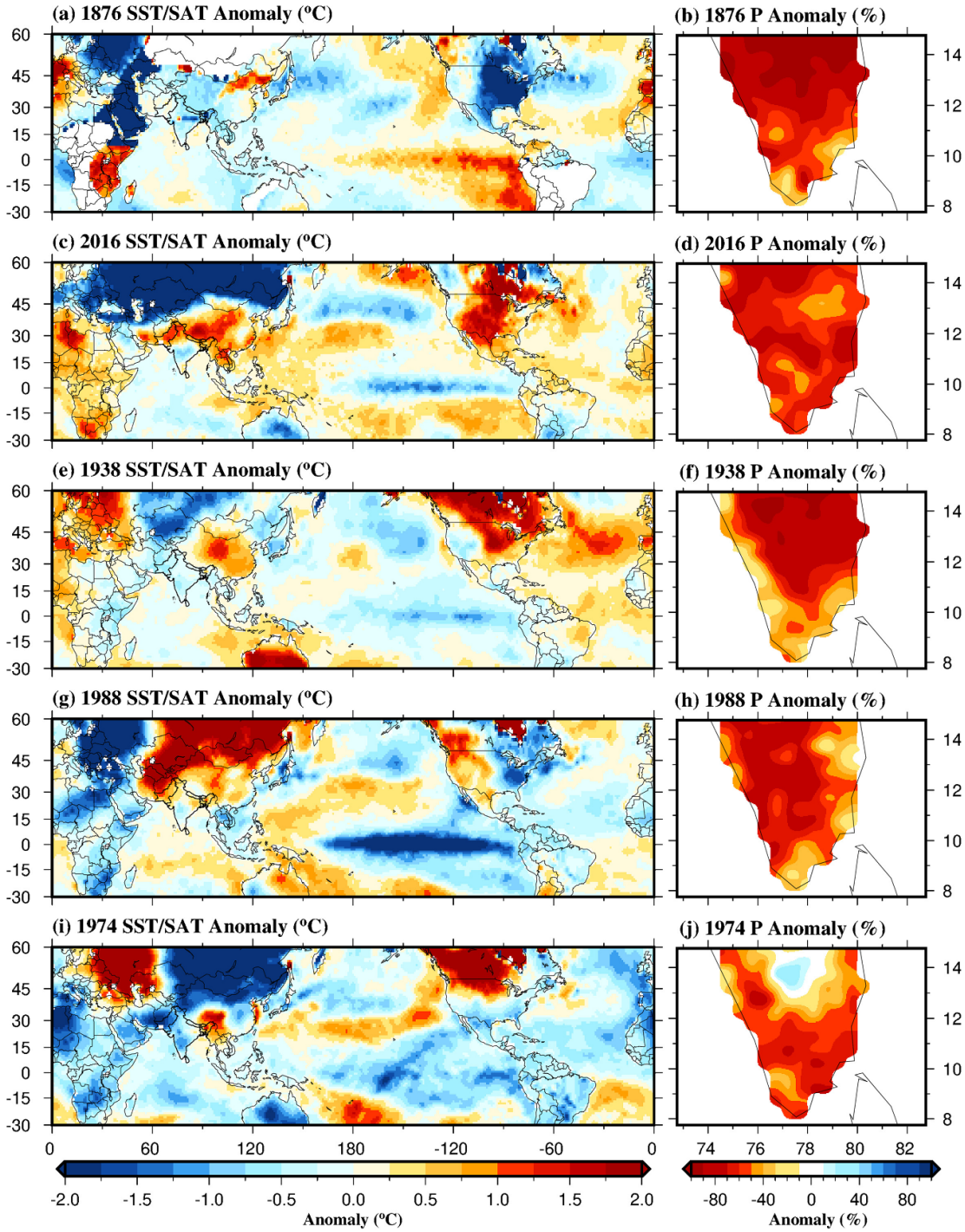

Figure 4. Sea surface temperature (SST)/surface air temperature (SAT) and precipitation (P) anomalies for the top five droughts that occurred in South India during the northeast monsoon for 1870–2018 period. SST and SAT datasets were obtained from Hadley Center and Berkley Earth, respectively. SAT data over few regions are not available for 1876.

1876–78 Great Drought on South Indian rainfall. Overall, the leading mode of SST and precipitation variability during the NEM shows that cold SST anomalies in the Indo-Pacific facilitate drought conditions over South India.

We performed EOF analysis to identify the dominant patterns of NEM rainfall in South India (figure 6). The first leading mode from the EOF analysis picks out rainfall variability across the entirety of South India and explains 50% of total variance (figure 6(a)). The second leading mode reveals a bipolar rainfall pattern across the northern and southern parts of South India and explains 11% of the total variance (figure 6). We note that the characteristics of rainfall variability derived from the first and second modes of EOF analysis are consistent with the leading modes obtained from the MCA (figure 5). Taken together, our findings inferred from both EOFs and MCA show that the first leading mode affects rainfall across South India, whereas the second

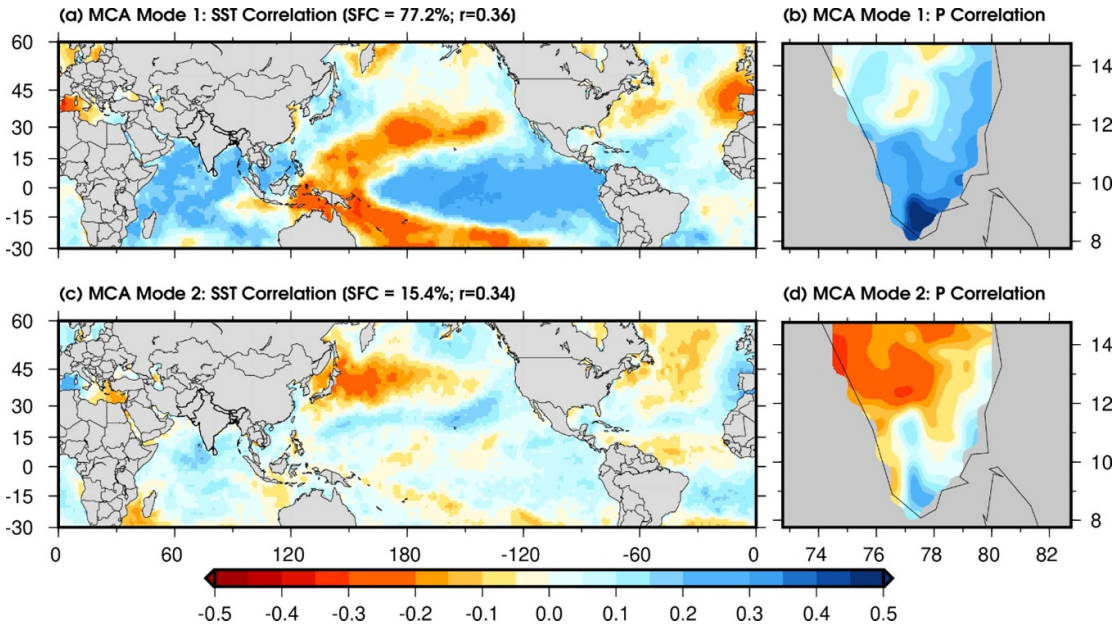

Figure 5. Links between South Indian precipitation and sea surface temperature (SST) during the Northeastern Monsoon season. (a), (b) Correlation patterns obtained from the first leading mode of maximum covariance analysis (MCA) performed between precipitation across South India (8°N–15°N and 74°E–81°E; see Green Box in figure 1) and SST during the October–November–December (OND) season over 1870–2018. (c), (d) Same as in the above panels but for the second leading mode of MCA. Rainfall was obtained from the IMD dataset whereas SST was retrieved from HadSST.

leading mode delineates opposing rainfall trends in the North versus the southern parts of South India (figure 6).

We calculated principal components (PCs) associated with the leading modes of variability derived from the EOF analysis (PC1 and PC2) to examine the predictability of NEM rainfall using SST anomalies (figure S8). We also computed the correlation between PC1 and SST anomalies in addition to oceanic indices (table S1) at different time lags (tables S2 and S3). We find that the first principal component (PC1) is strongly correlated ($r = 0.23$, P-value < 0.05) to SSTs from April–June (AMJ) in the Nino 3.4 region (figure 6). However, PC2 is more appropriately delineated by ($r = 0.33$, P-value < 0.05) SST anomalies from OND in Nino 3.4 and in the NIO (figure 6). We use this lagged relationship between oceanic indices and SST anomalies with PCs to establish a predictive model for NEM rainfall (as in Zhou *et al* 2019). Focusing on the first mode of variance, we used climatological Nino 3.4 SSTs from AMJ to predict rainfall in South India during OND (figure S9). We find that the OND rainfall is more skillfully predicted using AMJ Nino 3.4 anomalies in comparison to SST anomalies over OND NIO (figure S9). We also note that there is no significant increase in prediction skill when both AMJ Nino 3.4 and OND SST anomalies were used as opposed to Nino 3.4 SST anomalies alone (figure S9) due to high year-to-year variability between Nino 3.4 and NIO (figure S10). Overall, our analysis shows that SST anomalies at Nino 3.4 and over NIO can be used to predict rainfall during the NEM over South India with limited prediction skill.

4. Summary and conclusions

South India faced a severe water crisis during 2016–2018. In June 2019, a 'day zero' was declared in Chennai, Tamil Nadu, due to groundwater depletion and drying of four major reservoirs that supply water (Murphy and Mezzofiore 2019), largely induced by this event. We have shown that this extreme deficit was brought about by one of the worst droughts in the last 150 years. The 2016–2018 drought was worse than the 1874–1876 Great Drought, which was linked to the Great Madras famine and the deaths of several million in South India (Mishra *et al* 2019). The severity of the 2016–18 event during the NEM season peaked in 2016—the second singular driest year on record (after 1876). Dynamically, our study implicates negative IOD and La Niña conditions as facilitators for NEM rainfall deficits, where landward moisture transport from the Bay of Bengal into peninsular India is inhibited. The prevalence of La Niña throughout 2016 and 2017 (DiNezio *et al* 2017) further worsened the drought that started in 2016. Such rainfall deficits over consecutive years can result in multi-year drought, which have substantial and adverse impacts on surface and groundwater storage, and profoundly affect water availability and agriculture in the densely populated South Indian region. Although the intensity and timing of this recent event raise the possibility of anthropogenic forcing influencing NEM droughts, future work focusing on detection and attribution is required to separate the influence of natural variability (Thirumalai *et al* 2017, Williams *et al* 2020, Winter *et al* 2020). Moreover,

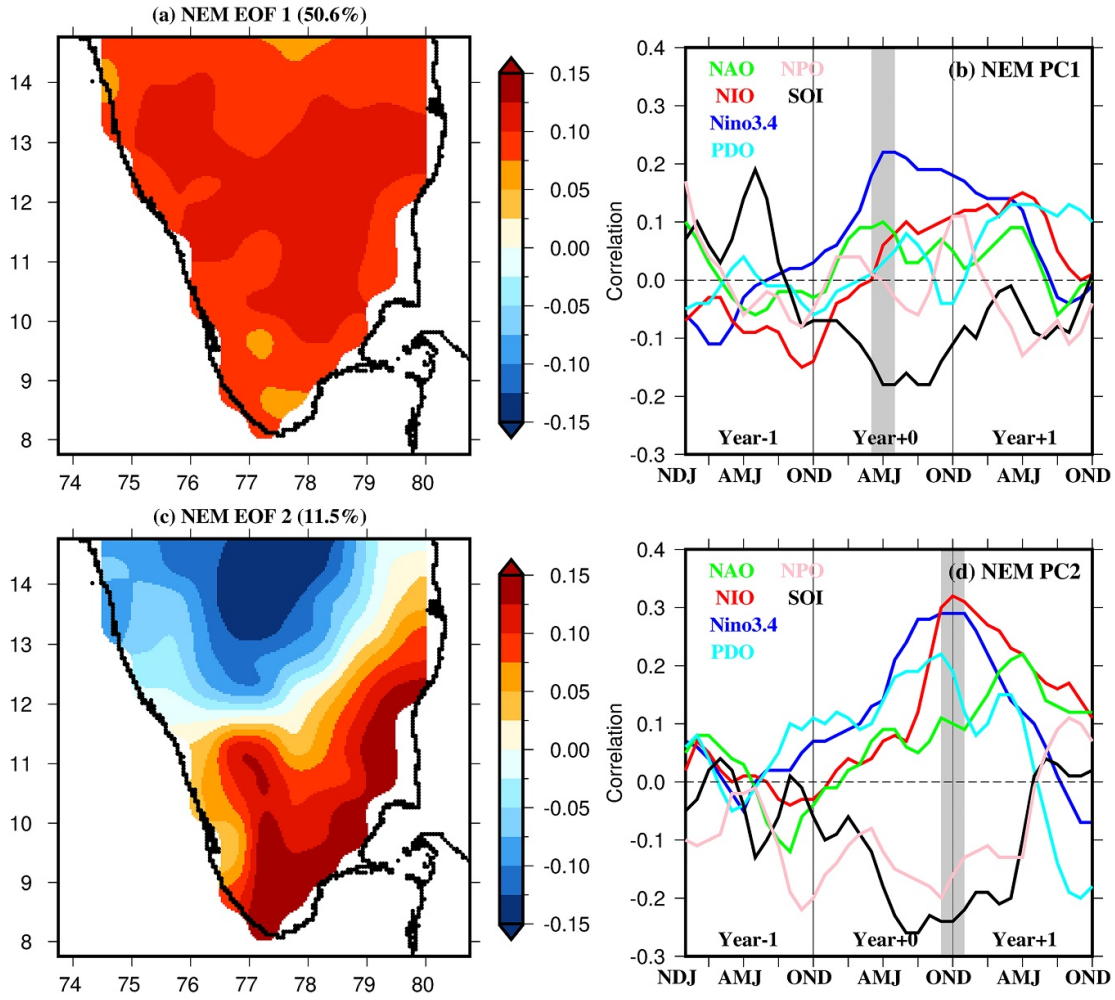

Figure 6. The leading modes obtained from the empirical orthogonal function (EOF) analysis of rainfall during the NEM for the 1870–2018 period. (a) The first leading EOF mode of NEM, which explains 50.6% of the total variance in NEM rainfall in South India. (b) Lagged correlation between the first leading principle component (PC 1) and 3-month mean SST anomalies over different regions (Nino 3.4 (5°S–5°N, 120–170°W), North Indian Ocean (NIO; 6°–24°N, 40–100°E), North Pacific Ocean (NPO; 30°N–50°N, 120°E–175°W), North Atlantic Ocean (NAO; 6°–24°N, 10–60°W), Pacific Decadal Oscillation (PDO), and Southern Oscillation Index (SOI)). (c) and (d) same as (a) and (b) but for the second leading EOF mode and the corresponding PC 2. Year − 1, Year + 0, and Year + 1 represent the previous, current, and next year of the NEM season, respectively.

potential changes in future patterns of SST variability in the Indian Ocean and tropical Pacific will add substantial uncertainty to projections and prediction of NEM rainfall.

Data availability statement

The data that support the findings of this study are available upon reasonable request from the authors.

Acknowledgments

We acknowledge the India Meteorological Department for providing the precipitation data. The last author appreciates financial assistance from the Indian Ministry of Human Resource Development (MHRD). The study is partially funded by the Ministry of Earth Sciences and Ministry of Water Resources forum projects. KT was supported by NSF Grant No. OCE-1903482 and acknowledges the University of Arizona and the Department of Geosciences for support.

ORCID iDs

Vimal Mishra https://orcid.org/0000-0002-3046-6296
Kaustubh Thirumalai https://orcid.org/0000-0002-7875-4182
Saran Aadhar https://orcid.org/0000-0003-1645-4093

References

Aguilera J 2019 Water is running out in this Indian City, causing crisis *Time* (available at: https://time.com/5611385/india-chennai-water-crisis/)
Ashok K, Guan Z and Yamagata T 2001 Impact of the Indian Ocean dipole on the relationship between the Indian monsoon rainfall and ENSO *Geophys. Res. Lett.* **28** 4499–502

Asoka A, Gleeson T, Wada Y and Mishra V 2017 Relative contribution of monsoon precipitation and pumping to changes in groundwater storage in India *Nat. Geosci.* **10** 109–17

Aulong S, Chaudhuri B, Farnier L, Galab S, Guerrin J, Himanshu H and Prudhvikar Reddy P 2012 Are South Indian farmers adaptable to global change? A case in an Andhra Pradesh catchment basin *Reg. Environ. Change* **12** 423–36

Barlow M, Cullen H and Lyon B 2002 Drought in Central and Southwest Asia: La Niña, the warm pool, and Indian Ocean precipitation *J. Clim.* **15** 697–700

Blanford H F 1884 II. On the connexion of the Himalaya snowfall with dry winds and seasons of drought in India *Proc. R. Soc.* **37** 3–22

Bretherton C S, Smith C and Wallace J M 1992 An intercomparison of methods for finding coupled patterns in climate data *J. Clim.* **5** 541–60

Cai W *et al* 2018 Increased variability of eastern Pacific El Niño under greenhouse warming *Nature* **564** 201–6

Castle S L, Thomas B F, Reager J T, Rodell M, Swenson S C and Famiglietti J S 2014 Groundwater depletion during drought threatens future water security of the Colorado River Basin *Geophys. Res. Lett.* **41** 5904–11

Census of India 2011 Website: office of the registrar general & census commissioner, India (available at: http://censusindia.gov.in/2011-Common/CensusData2011.html) (Accessed 27 April 2020)

Chennai water crisis: City's reservoirs run dry *BBC News* (available at: www.bbc.com/news/world-asia-india-48672330) (Accessed 18 June 2019)

Christensen J H *et al* 2013 IPCC 2013 chapter 14: climate phenomena and their relevance for future regional climate change supplementary material *Climate Change 2013: The Physical Science Basis. Contribution of Working Group I to the Fifth Assessment Report of the Intergovernmental Panel on Climate Change* p 62 (https://doi.org/10.1017/CBO9781107415324.028)

Cook E R, Anchukaitis K J, Buckley B M, D'Arrigo R D, Jacoby G C and Wright W E 2010 Asian monsoon failure and megadrought during the last millennium *Science* **328** 486–9

Dimri A P, Yasunari T, Kotlia B S, Mohanty U C and Sikka D R 2016 Indian winter monsoon: present and past *Earth–Sci. Rev.* **163** 297–322

DiNezio P N *et al* 2017 A 2 year forecast for a 60–80% chance of La Niña in 2017–2018 *Geophys. Res. Lett.* **44** 11624–35

Gadgil S and Gadgil S 2006 The Indian monsoon, GDP and agriculture *Econ. Political Wkly.* **41** 4887–95 (www.jstor.org/stable/4418949)

Hersbach H and Dee D 2016 ERA5 reanalysis is in production *ECMWF Newslett.* **147** 5–6

Kripalani R H and Kulkarni A 1997 Rainfall variability over South-East Asia—connections with Indian monsoon and Enso extremes: new perspectives *Int. J. Climatol.* **17** 1155–68

Kripalani R H and Kumar P 2004 Northeast monsoon rainfall variability over south peninsular India vis-à-vis the Indian Ocean dipole mode *Int. J. Climatol.* **24** 1267–82

Kumar P, Rupa Kumar K, Rajeevan M and Sahai A K 2007 On the recent strengthening of the relationship between ENSO and northeast monsoon rainfall over South Asia *Clim. Dyn.* **28** 649–60

Long D, Scanlon B R, Longuevergne L, Sun A Y, Fernando D N and Save H 2013 GRACE satellite monitoring of large depletion in water storage in response to the 2011 drought in Texas *Geophys. Res. Lett.* **40** 3395–401

Mishra A K and Singh V P 2010 A review of drought concepts *J. Hydrol.* **391** 202–16

Mishra V 2020 Long-term (1870–2018) drought reconstruction in context of surface water security in India *J. Hydrol.* **580** 124228

Mishra V, Cherkauer K A and Shukla S 2010 Assessment of drought due to historic climate variability and projected future climate change in the Midwestern United States *J. Hydrometeorol.* **11** 46–68

Mishra V, Smoliak B V, Lettenmaier D P and Wallace J M 2012 A prominent pattern of year-to-year variability in Indian Summer Monsoon Rainfall *Proc. Natl Acad. Sci. USA* **109** 7213–7

Mishra V, Tiwari A D, Aadhar S, Shah R, Xiao M, Pai D S and Lettenmaier D 2019 Drought and famine in India, 1870–2016 *Geophys. Res. Lett.* **46** 2075–83

Mo K C 2011 Drought onset and recovery over the United States *J. Geophys. Res. Atmos.* **116** 20

Murphy P P and Mezzofiore G 2019 Chennai water shortage: India's 6th-largest city is almost out of water. Satellite images show bone-dry reservoirs (available at: https://edition.cnn.com/2019/06/20/world/chennai-satellite-images-reservoirs-water-crisis–trnd/index.html) (Accessed 27 April 2020)

Niranjan Kumar K, Rajeevan M, Pai D S, Srivastava A K and Preethi B 2013 On the observed variability of monsoon droughts over India *Weather Clim. Extremes* **1** 42–50

Pai D S, Sridhar L, Rajeevan M, Sreejith O P, Satbhai N S and Mukhopadyay B 2014 Development of a new high spatial resolution (0.25° × 0.25°) long period (1901–2010) daily gridded rainfall data set over India and its comparison with existing data sets over the region *Mausam* **65** 1–18

Rajeevan M, Unnikrishnan C K, Bhate J, Niranjan Kumar K and Sreekala P P 2012 Northeast monsoon over India: variability and prediction *Meteorol. Appl.* **19** 226–36

Rayner N A *et al* 2003 Global analyses of sea surface temperature, sea ice, and night marine air temperature since the late nineteenth century *J. Geophys. Res.* D **108** 14

Rohde R, Muller R A, Jacobsen R, Muller E and Wickham C 2013 A new estimate of the average earth surface land temperature spanning 1753–2011 *Geoinfor. Geostat.: Overview* **1**

Roxy M K, Ritika K, Terray P, Murtugudde R, Ashok K and Goswami B N 2015 Drying of Indian subcontinent by rapid Indian Ocean warming and a weakening land-sea thermal gradient *Nat. Commun.* **6** 1–10

Samaniego L *et al* 2018 Anthropogenic warming exacerbates European soil moisture droughts *Nat. Clim. Change* **8** 421–6

Singh D, Ghosh S, Roxy M K and McDermid S 2019 Indian summer monsoon: extreme events, historical changes, and role of anthropogenic forcings *Wiley Interdiscip. Rev. Clim. Change* **10** e571

Singh D, Seager R, Cook B I, Cane M, Ting M, Cook E and Davis M 2018 Climate and the Global Famine of 1876–78 *J. Clim.* **31** 9445–67

Thirumalai K, DInezio P N, Okumura Y and Deser C 2017 Extreme temperatures in Southeast Asia caused by El Ninõ and worsened by global warming *Nat. Commun.* **8** 1–8

Thomas B F, Caineta J and Nanteza J 2017 Global assessment of groundwater sustainability based on storage anomalies *Geophys. Res. Lett.* **44** 11445–55

Timmermann A *et al* 2018 El Niño–Southern Oscillation complexity *Nature* **559** 535–45

Van Loon A F 2015 Hydrological drought explained *Wiley Interdiscip. Rev.* **2** 359–92

Wiese D N, Landerer F W and Watkins M M 2016 Quantifying and reducing leakage errors in the JPL RL05M GRACE mascon solution *Water Resour. Res.* **52** 7490–502

Williams A P *et al* 2020 Large contribution from anthropogenic warming to an emerging North American megadrought *Science* **368** 314–8

Winter J M, Huang H, Osterberg E C and Mankin J S 2020 Anthropogenic impacts on the exceptional precipitation of 2018 in the Mid-Atlantic United States *Bull. Am. Meteorol. Soc.* **101** S5–S10

Wu Z and Huang N E 2009 Ensemble empirical mode decomposition: a noise-assisted data analysis method *Adv. Adapt. Data Anal.* **1** 1–41

Wu Z, Huang N E, Wallace J M, Smoliak B V and Chen X 2011 On the time-varying trend in global-mean surface temperature *Clim. Dyn.* **37** 759–73

Yadav R K 2012 Why is ENSO influencing Indian northeast monsoon in the recent decades? *Int. J. Climatol.* **32** 2163–80

Zhou Z, Xie S and Zhang R 2019 Variability and predictability of indian rainfall during the monsoon onset month of June *Geophys. Res. Lett.* **46** 14782–8

Zubair L and Ropelewski C F 2006 The strengthening relationship between ENSO and northeast monsoon rainfall over Sri Lanka and southern India *J. Clim.* **19** 1567–75